

## **Melting in the crust and upper mantle beneath the Kenya Rift: evidence from Geomagnetic Deep Sounding experiments**

Banks, R.J. & Beamish, D., 1979. Melting in the crust and upper mantle beneath the Kenya Rift: evidence from geomagnetic deep sounding experiments. *Journal of the Geological Society, London*, 136, 225-233.

doi: 10.1144/gsjgs.136.2.0225

R.J. Banks, Department of Environmental Sciences, University of Lancaster, Bailrigg, Lancaster.  
D. Beamish, Geomagnetism Unit. Institute of Geological Sciences, Murchison House, West Mains Road, Edinburgh.

**SUMMARY:** A Geomagnetic Deep Sounding experiment in and around the Kenya Rift Valley has shown that telluric currents are concentrated by 3 regions with high electrical conductivity. Two of the anomalies are related to the rift structure, and the combination of different lines of geophysical evidence strongly suggests that the high conductivity is due to the presence of molten material in the rocks of the lower crust and upper mantle. The shallower zone where melt is present is located directly beneath the floor of the rift valley. Its upper surface is no deeper than 20 km; it may be as shallow as 5 km. The electrical conductivity is compatible with an average melt concentration of 5-10%, but could also be explained by discrete magma chambers where the concentration was much higher. The deeper conductor is located to the E of the rift valley beneath the Aberdare Mountains, and possibly extends beneath Mount Kenya. The Geomagnetic Deep Sounding data suggest a depth of 100 km to the high conductivity body, which appears to correspond to the core (the region with the highest melt concentration) of a zone of more diffuse melting in the mantle, that is responsible for seismic and regional gravity anomalies, and which supports a part of the topographic elevation of the Kenya dome.

Although the electrical conductivity is a difficult and often ambiguous physical property of the Earth to interpret, it can provide very valuable insights into the physical state of the crust and upper mantle. We have used the Geomagnetic Deep Sounding method to investigate the electrical conductivity beneath the East African rift system in Kenya. The data processing techniques have been optimized so as to obtain the maximum of useful information from the data, while making the smallest possible number of assumptions. It is clear from the results that the conductivity structure around the rift valley is three-dimensional; however, the methods of analysis enable us to select those parts of the structure, and that part of our data, that can be justifiably modelled by a two-dimensional structure. The coverage of the eastern rift by other geophysical techniques has been relatively thorough, and the interpretation of the physical significance of the conductivity anomalies must be compatible with estimates of other physical properties such as seismic velocity and density. When the interpretation is constrained in this way, the GDS experiment yields information which should prove to be of great value in the synthesis of tectonic and petrogenetic models of the rift system.

### **Anomalous magnetic fields and internal currents**

#### *The analysis of GDS data*

In GDS experiments, records are made at an array of closely-spaced points on the Earth's surface, of time variations of the geomagnetic field. The fluctuating fields are partly of external origin, generated by currents in the ionosphere and magnetosphere, and partly of internal origin, caused by currents induced in the more conducting parts of the Earth by the external field variations. The usual aim of GDS experiments is to detect departures from the 'normal', spherically symmetric, global conductivity distribution. The additional internal fields created by the lateral heterogeneity are referred to as 'anomalous'; to distinguish them from 'normal' internal fields generated by the currents induced in the spherically symmetric conductivity structure.

The first stages in the analysis of GDS data are aimed at separating the anomalous internal part from the measured magnetic field. The geometry of the anomalous fields is controlled (at least in part) by the internal conductivity structure of the Earth. In consequence, consistent relationships exist between different components of the anomalous field. Thus, we can estimate the anomalous internal field by separating out that part of a magnetic field component at a particular site which shows a persistent relationship to another component, either at the same or at a different location. The details of the techniques used to achieve this separation are described by Beamish (1977).

In the analysis of the effects of relatively small-scale conductivity anomalies on the electromagnetic field, we assume that the main effect of the anomaly is to perturb a regional flow of current, that originated by induction in some much larger conductor elsewhere: possibly in the oceans, or in the normal conductivity distribution. If the structure is two-dimensional, its electromagnetic response is completely characterised by the anomalous fields produced by just one azimuth of the regional current flow (provided the strike of the structure is known). Usually, we choose to define the response in terms of the anomalous fields produced when the regional current flow is parallel to the strike of the conductor, since their amplitude is then a maximum. When the structures are three-dimensional, the anomalous fields produced by 2 orthogonal azimuths of regional current flow are required to define the response of the anomaly. If a conductor is sufficiently elongated, one particular azimuth of current flow should maximise the fields near the centre, while the orthogonal azimuth should give rise to no anomalous fields. Such behavior is one indication that a profile across the centre of the conductor can be interpreted in terms of a two-dimensional structure.

The response of electromagnetic induction anomalies may be frequency-dependent. In anticipation of such effects, it is usual practice as the very first step to analyse magnetic variation data into

frequency bands. The frequency dependence of the anomalous fields may provide additional constraints on models of the conductivity structure. The Kenya data has been analysed into 6 bands, covering periods of 512-128, 128-64, 64-32, 32-16, 16-8, and 8-4 min. They are referred to as bands 1 to 6 respectively.

### *Anomalous magnetic variations in Kenya*

The distribution of magnetometers operated in our experiment is shown in Fig. 1, relative to the major faults that delineate the rift valley in Kenya. At each of these stations, the response to a regional horizontal magnetic field with a general azimuth has been computed. To display the spatial structure of the anomalous fields, a particular azimuth is selected, and the anomalous fields calculated at each station in turn. These predicted fields are then interpolated on to a regular grid, so that a contour map can be created. In some parts of the resultant map, the contours are poorly determined because of the inadequacy of the original station distribution. Such areas are indicated by dashed contours. The maps (Fig. 2-4) show the amplitude or phase of a component of the anomalous field produced around the rift valley when the horizontal field at Homa Bay (HBY) or Kisii (KSI) in the extreme W of the survey area, has unit amplitude and specified azimuth. In Figs. 2 and 3, the azimuth of the regional horizontal magnetic field is  $60^\circ\text{E}$ ; we expect the azimuth of the regional current flow to be  $150^\circ\text{E}$ . Beamish (1977) has described how different features of the anomalous fields respond to changes in the chosen azimuth. Two groups of structures can be distinguished. North of  $1^\circ\text{S}$ , the structures in the maps show two-dimensional behavior. There is a very definite maximum and minimum in the response at 2 orthogonal azimuths of the regional field, and the minimum is very close to zero. The maximum response occurs when the regional current flow is directed NNW-SSE, parallel to the strike of the rift faults. In the SE of the survey area, around Nairobi (NBI), anomalies are present in the maps whatever the azimuth of the regional field, suggesting that the conductivity structure is three-dimensional. The maximum response is to a regional current striking  $150^\circ\text{E}$ . Thus, by displaying the response of the area as a whole for this azimuth, we are showing both groups of anomalies to very nearly maximum effect.

The distribution of internal currents is not uniquely determined by surface measurements of the magnetic field, and it is necessary to restrict possible current models in some way. A convenient assumption is to suppose that the currents are confined to a thin sheet at a specified depth; the current density in the sheet is then uniquely determined by the surface fields. If the current in the sheet is concentrated in a narrow strip (a line current) the vertical field directly above will be zero, and it will be a maximum to either side of the current; moreover, the phase of the vertical field changes by  $180^\circ$  as the current is crossed. The component of the horizontal field perpendicular to the strike of the current will be a maximum directly above it. If the current is not so localised, but forms a more diffuse sheet, the vertical field maximum is to one side of the sheet, and the horizontal field is enhanced over the entire sheet.

These ideas provide the necessary background to the interpretation of Figs. 2 to 4. In Fig. 2, there is a change in the sign of the vertical field as the rift valley is crossed from W to E. The zero contour lies on the E side of the rift at the equator, but strikes NW-SE away from the rift at  $10^\circ\text{S}$ . The amplitude of the vertical field is greatest to either side of this contour, but the pattern is not symmetric; to the W and SW, the maximum amplitude is 0.3 to 0.5- to the E and NE it is only 0.1. Such a pattern is more complex than that to be expected from either the line current or sheet model. However, a combination of the two, with a line current beneath the rift, and a sheet extending some distance eastwards from the rift would explain the observations.

An examination of the phase of the vertical field (Fig. 3) reveals a similar picture. At the equator, the contours strike approximately N-S, and as the rift is crossed the phase changes from  $-170^\circ$  in the

W to  $+120^\circ$  in the E. Such a change cannot be produced by a simple line current ; the total change ought to be  $180^\circ$ . Near Nairobi (NBI), the contours run NW-SE, and the phase change along a line perpendicular to them is close to  $180^\circ$ . The implication is that a single current flows in a SE-NW direction between Nairobi and Thika (TKA). The complex behavior of the phase further N can only be explained if there are 2 conductors, one of which is sufficiently large to modify the phase of the internal currents by means of its self-inductance. A final point of interest is the E-W strike of the contours at  $1^\circ\text{S}$ , suggesting that current is jumping across from the conductor in the SE to a conductor beneath the rift valley.

Figure 4 shows the amplitude of the horizontal E component of the magnetic field that is created by a regional current flow in the N-S direction . The magnetic field displayed is the *total* E component; i.e. the sum of the normal and anomalous parts. Consequently, its expected value, in the absence of anomalies, is one. Departures from this value are caused by anomalous currents which have an N-S component of flow. The enhancement of the E component above and to the E of the rift, N of  $1^\circ\text{S}$ , is very noticeable. It indicates that the regional N-S currents are being concentrated beneath and to the E of the rift by a conducting body striking approximately N-S. The presence of the Nairobi anomaly, striking NW-SE, shows that a conductor with that azimuth is also deflecting and concentrating the northward flowing current. The gap in the contours at  $1^\circ\text{S}$ , between the rift anomaly and the Nairobi anomaly, is probably real. It shows that the current flow in this region has been turned  $90^\circ$  into an E-W direction, and that current channeled through the southeastern conductor is being fed across into the rift conductor, in agreement with the interpretation of the vertical component phase data.

#### *The configuration of the conductors*

The discussion in the previous section suggested the existence of 3 conductors in the area we investigated.

(i) A conductor beneath the floor of the rift valley, running northward out of the survey area. There is evidence that it extends no further than  $1^\circ\text{S}$ . It certainly does not extend any significant distance W of the western wall of the rift valley, and the behavior of the anomalous fields at Thomson's Falls (TFL), on the eastern margin of the rift, shows that the conductor is similarly limited by the eastern wall of the rift (Beamish 1977). The lateral confinement of the conductor to the region directly beneath the floor of the graben, has been confirmed by magnetotelluric measurements made at a series of stations along an equatorial profile (Rooney & Hutton 1977). The maximum possible depth of the upper surface of the conductor can be estimated from the spatial gradients of the anomalous fields along the same profile: it turns out to be 20 km (Beamish 1977). The magnetotelluric data extend to higher frequencies than our GDS data, and consequently impose tighter limits on the depth of the conductor. They require that almost the entire crust, from close to the surface to depths of more than 35 km, should be conducting (Rooney & Hutton 1977). The strike of this conductor is parallel to the rift structures S of the equator. At periods less than 30 min, along an equatorial profile, it responds in the manner to be expected of a two-dimensional structure.

(ii) A conductor located slightly to the E of the rift valley. It too strikes parallel to the rift structures, and probably extends no further than  $1^\circ\text{S}$ . Its precise lateral extent is difficult to determine because of the complex interaction between the fields generated by conductors (i) and (ii). The spatial gradients of the fields to the E of the rift are smaller than those immediately to the W, suggesting that this second conductor is deeper than the first.

(iii) A conductor running SE to NW between Nairobi and Thika. It extends southeastwards out of the survey area, but is truncated by the rift structures. The steep gradients of the fields indicate a shallow source, probably within the crust.

## Conductivity models

The evidence suggests that a two-dimensional model can be justified for the observations made N of  $1^{\circ}$ s. However, stations further S detect anomalous fields at all azimuths of the regional current flow. Consequently, the use of a two-dimensional structure to model the response of the 'equatorial' stations is most likely to be valid for the shorter period magnetic field variations. The skin-depth of variations with periods greater than 30 min, in bodies whose conductivity is  $10^{-1} \text{ S.m}^{-1}$ , is more than 50 km. The distance of the equatorial line from the southern limit of the conductors is probably 80 to 100 km, or not much more than the skin-depth. At a distance of only one skin-depth from the end of the conductor, the discrepancy between the true response and that calculated for the equivalent two-dimensional model cannot be ignored. We should, therefore, not attempt to fit the observed response of the equatorial line at any period greater than 30 min. Even at this period, the end of the conductor is only 2 skin-depths away, and we must still expect some effect on the observed response.

The data that we have tried to fit by a two-dimensional model is the response at stations on, or close to, an approximately equatorial line, perpendicular to the strike of conductors (i) and (ii). Three different measures of the response have been employed. The first, used in the initial attempts, is the single-station 'maximum' response, introduced by Banks & Ottey (1974). It is the ratio (amplitude and phase) of the anomalous internal vertical field to the total horizontal field perpendicular to the strike of the conductor. The magnitude of the response is a maximum when the regional current flow is parallel to the strike of the conductor, and it is this maximum value that we attempt to model. A preferable response measure is the ratio of the vertical field at a given station to the regional horizontal field. These 'inter-station' response estimates were used as checks on the validity of the preferred models. Finally, we were also able to compute the ratio of the total E magnetic component at each station to the regional E component. The maximum value of this response is associated with N-S regional currents.

The arguments outlined in the section on 'The configuration of the conductors' formed the basis for the initial choice of conductivity model. Numerous experiments led us eventually to a model of the kind shown in Figs. 5 and 6, involving 2 highly conducting regions. The first, located beneath the rift at depths of 20 to 35 km, has a conductivity of  $10^{-1} \text{ S.m}^{-1}$ . Our data are limited to relatively low frequencies (only periods longer than 8 min gave really reliable results), and even near the rift valley the station spacing is 30 km or more. Consequently, we cannot resolve in detail the conductivity structure in the depth range 0 to 40 km. The data do constrain the product of the conductivity and thickness of the sub-rift conductor, and we can also be confident that the top of the body is no deeper than 20 km. However, as far as our measurements are concerned, it could equally well extend from the surface downwards. Indeed, the magnetotelluric measurements have shown that the upper crust is also conducting. Rooney & Hutton (1977) found conductivities of  $10^{-1} \text{ S.m}^{-1}$  from the surface to depths of more than 35 km. Like us, they were not able to determine the precise details of the vertical conductivity profile. However, they were confident that some conducting material must be present no more than 5 km below the surface, and some must also be present at depths down to 35 km.

The second conductor, to the E of the rift, is much deeper. The depth of the upper surface shown in Fig. 5 is 150 km, but any value greater than 100 km gives a satisfactory fit to the observed profile. The conductivity is slightly lower:  $5 \times 10^{-2} \text{ S.m}^{-1}$ . The lateral extent of the eastern conductor is most strongly constrained by the horizontal field response shown in Fig. 6, and cannot much exceed 100 km, as shown. Its western boundary is not well-determined, because of the juxtaposition of the two conductors; they may well overlap to some extent.

The model in Figs. 5 and 6 is similar in its general features to that proposed by Banks & Ottey (1974). However, it differs significantly in that the eastern conductor is located considerably deeper (more than 100 km, as opposed to 50 km), and its eastward extent has been greatly reduced (from 400 to 100 km). These changes have been occasioned by the tighter constraints provided by the larger number of stations, and the inter-station and horizontal component response estimates.

#### *Geophysical significance of the conductivity anomalies*

The electrical conductivity of rocks is influenced by many factors, and if a meaningful interpretation of the conductivity model is to be made, the constraints imposed by other geophysical data must be used to establish the mechanism responsible for the high conductivity we have detected. In assessing the information from other geophysical methods about the physical state and composition of the crust and mantle, we shall concentrate on 2 regions: the lower crust and uppermost mantle beneath the rift valley between 2°N and 2°S, and the deeper mantle beneath and immediately to the E of the rift valley. The conductor between Nairobi and Thika is not discussed any further in this paper. There are no other geophysical data to support the existence of a NW-SE trending structure there, though it is parallel to basement lineaments, and seems to represent a continuation of one of the major faults bounding the eastern margin of the rift valley. However, it is possible that what we have interpreted as a separate conductor is really a complex current channeling effect associated with the southern boundary of the other 2 conductors.

#### *Shallow structure beneath the rift valley*

Seismic and gravity investigations have shown that the crust beneath the floor of the rift valley is quite distinct from that beneath the immediate flanks. The crustal thickness on the flanks is in the range 42-46 km, and seismic P-wave velocities are 5.8-6.5 km.s<sup>-1</sup> (Maguire & Long 1976). Beneath the floor of the rift, however, velocities of 6.4 km.s<sup>-1</sup> have been found at a depth of only 3 km (Griffiths *et al.* 1971), and there is evidence that the velocity increases to 7.1-7.5 km.s<sup>-1</sup> at 20 km depth (Griffiths *et al.* 1971, Maguire & Long 1976). These results may not be representative of the entire rift valley, but it is clear that at least sections of the crust beneath the rift floor are composed of rocks whose seismic velocity is significantly greater than that of the crust beneath the flanks at the same depth.

The high velocity material within the rift crust also has a high density relative to the surrounding rocks, and gives rise to a positive gravity anomaly. The mapping of this anomaly yields a more detailed picture of the width, continuity and relationship to the surface geology of the anomalous crustal material. The anomaly extends more or less continuously from 2°S to 2°N, following the western side of the rift depression from 2°S to the equator, and the eastern side from the equator to 2°N. There is no obvious extension beyond the limits of 2°S and 2°N. Unfortunately, the form of the gravity anomaly depends a good deal on the procedure used to separate it from the negative regional anomaly on which it is superimposed, and interpretations of the structure responsible for the anomaly vary considerably in detail (e.g. Searle 1970, Baker & Wohlenberg 1971, Fairhead 1976). The source is usually assumed to be either a massive intrusion with a width of about 10 km, or a broader zone of dyke injection; a contribution has also been attributed to dense lavas infilling the graben.

The seismic velocity models suggest that the source of the positive gravity anomaly is located in the depth range 3 to 20 km. Some clues to the rock types likely to occur at these depths are provided by the blocks and bombs of gabbro within flows of alkali basalt from Silali volcano, located at 1°N on the eastern side of the graben, above the axis of the gravity anomaly (McCall 1970). McCall believes their provenance is a shallow intra-crustal magma chamber, from which they have been detached by

gas coring. Phonolite and trachyte flows contain similar enclaves of syenite. Rocks with densities in the range 2800-3100 kg.m<sup>-3</sup> are needed to produce the measured seismic velocities. Both gabbro and syenite meet this requirement, though the higher velocities and densities are probably only compatible with gabbro. Direct geophysical evidence for the existence of intra-crustal magma chambers beneath the rift valley floor, or for high melt concentrations at crustal depths, is sparse. Seismic waves that propagate across the rift N of 1°S are very much attenuated relative to those that follow non-rift paths (Gurbuz 1974). Heat flow values in the rift valley are often high (Morgan 1974), but individual measurements show considerable scatter, no doubt due to the presence of hot water and steam circulating through cracks and pores in the crust. Because of the contribution made by such mechanisms to the process of heat transfer, it is not possible to infer the sub-rift temperature structure with a high degree of confidence from the heat flow data.

The geological and geophysical constraints that we have discussed considerably narrow the range of feasible explanations of the high conductivity zone detected beneath the rift floor by the GDS experiment. The possibilities are: electrolytic conduction through saline interstitial fluids in the rocks which immediately underlie the rift valley floor; or, at deeper levels, the enhanced conductivity which accompanies melting; or some combination of the two, since they are likely to be intimately associated. The latter possibility is supported by the magnetotelluric results (Rooney & Hutton 1977), which indicate that the entire crust, from close to the surface to depths of at least 35 km, is conductive. However, we believe that the major contribution to the GDS anomaly at periods of 16-32 min comes from melting at depths in excess of 10 km.

#### *Upper mantle structure beneath the dome*

In the vicinity of the equator, the East African Rift is divided, and runs across a plateau with an average elevation of 1000 m. The Kenya Rift Valley traverses an elliptical highland region approximately 500 km long and 300 km wide, with an average height of more than 2000 m, often referred to as the Kenya 'dome'. A number of authors have suggested that a significant part of the topography of the dome has been created by recurring episodes of 'domal uplift', related to the existence of thermal anomalies in the mantle (Baker *et al.* 1972). The evidence for the uplift comes from studies of the present-day elevation of erosion surfaces and bevels of different ages. Differences of opinion have arisen over the form and significance of the sub-volcanic surface, and the most recent work (King 1978) suggests that much of the present elevation of the basement was inherited from pre-rift up-arching, though late uplift of the rift shoulders must have occurred.

Banks & Swain (in prep.) have taken a different approach to the problem of establishing the fraction of topography that may have been created by thermal anomalies in the upper mantle. They show that there is a high coherence between Bouguer gravity anomalies and topographic features whose spatial scales exceed 200 km, and argue that the reason for the correlation is that the gravity anomalies represent the attraction of the low density material which compensates and supports the topography. The correlation with the gravity anomalies provides a means of separating out those components of the topography which are compensated, and the compensated topography, defined in this way, corresponds very well to the plateau and dome.

Evidence on the nature of the mechanism by which the topography is compensated has come from measurements of teleseismic P-waves recorded at the Kaptagat array (Long & Backhouse 1976), which have revealed the existence of a wedge of low velocity material in the mantle to the E of Kaptagat. Long & Backhouse (*op. cit.*) have presented their data in the form of 'slowness anomalies', plotted as vectors at the points where the corresponding seismic rays are believed to leave the low velocity prism. They point in the direction of thinning or deepening of the anomalous material, i.e.

away from the 'centre' of the anomaly. Fig. 7 shows that the vectors calculated by Long & Backhouse radiate from a point slightly to the E of the rift valley.

Material with low P velocity will also have a low density, and the anomalous zone should contribute to the compensation of the topography, and to the long wavelength gravity anomalies. Banks & Swain (in prep.) found that there is a considerable discrepancy between the gravity anomalies they infer for the compensation of the plateau and dome, and the anomaly to be expected for the low velocity material. However, they show that if the gravity anomaly of the compensation is further separated into a part associated with the plateau and a part associated with the dome, there is good correspondence between the dome anomaly and the seismic anomaly. Fig. 7 shows their estimate of the gravity anomaly of the material that supports the dome. The centre of the anomaly agrees well with the centre from which the slowness vectors radiate.

Although the gravity data probably provide the best two-dimensional picture of the extent of the mantle anomaly, they do not, on their own, tell us much about its depth or vertical extent. Seismic data are of only limited usefulness in setting stronger limits on the depth. Long *et al.* (1972) and Knopoff & Schlue (1972) measured the dispersion of surface waves propagating along paths that cross the dome. Inversion of the dispersion data shows that the shear wave velocity is anomalously low on *the* path at depths of 50 to 200 km. The average velocity required in this depth range is only  $4.25 \text{ km.s}^{-1}$ , compared with the normal mantle velocity of  $4.6 \text{ km.s}^{-1}$ . Unfortunately the data cannot discriminate between structures involving thick, moderately low velocity layers, and those with thinner, extremely low velocity layers. The Kaptagat teleseismic data suffer from somewhat similar difficulties. The calculated depth of the low velocity wedge depends upon the choice of velocity. In any case, Kaptagat is on the margin of the anomaly, and gives only poor control over the structure at the centre.

Banks & Swain (in prep.) have used the requirement that the topography of the dome should be isostatically compensated to establish tighter bounds on the vertical extent of the low density material. They deduced that at least 50% of the compensation of the dome must be shallower than 100 km. The average density reduction required between the base of the crust and 100 km must be at least  $25 \text{ kg.m}^{-3}$  and no more than  $50 \text{ kg.m}^{-3}$ . The average P and S velocities in this part of the mantle are  $7.3 \text{ km.s}^{-1}$  (Long & Backhouse 1976) or less, and  $4.25 \text{ km.s}^{-1}$  (Long *et al.* 1972). If the reduction in P velocity were due to a compositional difference or solid-solid phase change in the mantle, the velocity-density relationships deduced by Birch (1961) should be applicable. A seismic velocity drop of  $600 \text{ m.s}^{-1}$  relative to normal mantle should be associated with a density reduction of approximately  $200 \text{ kg.m}^{-3}$ . The discrepancy between this figure and the maximum density differences allowed by the gravity data forces us to conclude that the anomaly cannot be caused by a compositional or solid-solid phase change. The only plausible explanation of such large reductions in seismic velocity without a corresponding change in density is the presence of inclusions of molten material within the mantle rocks. The gravity and P-wave slowness anomalies plotted in Fig. 7 show that the region where the postulated zone of melting is thickest, or the melt concentration is greatest, approximately agrees with the position of the deep mantle conductivity anomaly.

#### *Interpretation of the conductivity anomalies*

The effects of melting on the bulk conductivity of rocks are discussed from both the experimental and theoretical points of view by Waff (1974). Laboratory measurements show that the conductivity of a tholeiitic melt is some 3-4 orders of magnitude higher than that of single crystal olivine at the same temperature. This may be taken as an indication of the conductivity contrast between the solid



matrix and the interstitial liquid in a partially molten upper mantle. Where the ratio of the conductivities is so large, the bulk conductivity of the rock is determined by the properties of the high conductivity phase, and is independent of those of the low conductivity phase. This is fortunate, because the conductivity of the melt, unlike that of the solid phase, is relatively insensitive to such factors as composition, oxygen fugacity, etc. Its conductivity does depend on the temperature.

Of greatest importance, however, is the dependence of the bulk conductivity of the rock on the melt concentration, and on the degree of connectivity of the individual melt pockets. The connectedness is itself a function of the melt concentration, but it is difficult to formulate a theoretical relationship between the two. When the melt concentration is low, the fraction of melt pockets that are linked is small, and the bulk conductivity is essentially that of the solid phase, i.e. very low. Once the melt concentration exceeds some critical value, such that more than 40% of the melt pockets are linked, the bulk conductivity rises very rapidly with only a small increase in melt concentration to a value of the same order as that of the liquid phase. If the geometry of the melt pockets is favourable, melt concentrations as low as a few % may be sufficient to cause this drastic increase in conductivity. When there is complete linkage of the melt pockets, or continuous wetting of the grains by the liquid phase, the bulk conductivity of the rock can be estimated using the approximate formula

$$\sigma^* \approx \frac{2}{3} c_m \sigma_m \quad (1)$$

where  $c_m$  is the melt concentration expressed as a fraction of the total volume, and  $\sigma_m$  is the melt conductivity, itself a function of the melt temperature.

On the basis of these considerations, we can see that there need not be an exact correspondence of the regions of high conductivity to the regions of low P velocity, S velocity and density. The bulk density and elastic properties of a rock that contains liquid inclusions do not show the critical dependence on the connectivity of the melt pockets that is characteristic of the conductivity (although the P and S velocities do depend on the shape of the melt pockets, as well as on the melt concentration (Anderson *et al.* 1972)). Quite low melt concentrations (e.g. less than 1%) can still produce significant reductions in the density and seismic velocities, even though they are too low to cause the critical jump in conductivity. The conductivity anomalies must therefore correspond to the regions in which the melt concentration is greatest, exceeding the critical value. Using Waif's (1974) data and equation (1), we can interpret our models in terms of the minimum melt fraction required to produce the estimated conductivity. If the melt temperature is 1200°C, a concentration of at least 5% is needed to produce the bulk conductivity of  $10^{-1} \text{ S.m}^{-1}$  which we inferred for the shallower conductor beneath the rift valley. The actual value could be higher if the linkage of the melt pockets is incomplete. A minimum concentration of 2 to 3% is required to explain the conductivity of the deep mantle anomaly ( $5 \times 10^{-2} \text{ S.m}^{-1}$ ). The interpretation of the GDS data suggests that the top of this anomaly lies at 100 km, yet the gravity data apparently require an average melt concentration *above* 100 km of at least 6%. The depth estimate from the GDS data may be unreliable, because of the use of a two-dimensional model to interpret a three-dimensional structure. Another possibility is that the critical melt concentration is greater than 6% due to a different melt geometry, and a correspondingly lower degree of connectivity.

These estimates of the melt fractions are based upon extremely crude conductivity models, which assume a uniform high conductivity within the anomaly and a uniform low value for the background. The existence of the critical threshold for the conductivity in response to increasing melt concentration makes this model less unrealistic than it would seem. However, it is highly probable that the melt concentration substantially exceeds our estimates in localised patches, and, particularly beneath the rift valley, the melt may be segregated into individual magma chambers.

## Conclusions

A geomagnetic deep sounding experiment in Kenya revealed the existence of 2 regions of high electrical conductivity associated with the rift valley. Through correlation with other geophysical data, we can interpret the high conductivity to be the result of melting in the lower crust and upper mantle. The GDS measurements can then be used to set limits on the position, lateral extent and melt fraction of the regions where the concentration exceeds a critical value of a few %.

One such region with this super-critical melt concentration is located at lower crustal depths, directly beneath the floor of the rift valley. It does not, apparently, extend further S than 1°S. An average melt concentration of 5-10% is required to match the inferred conductivity of  $10^{-1} \text{ S.m}^{-1}$ . The second highly conducting zone is centered to the E of the rift valley, and is significantly deeper. The lower conductivity suggests either a lower melt concentration or a lesser degree of connectivity of the melt pockets than is found beneath the rift floor.

ACKNOWLEDGEMENTS. We should like to thank the Natural Environment Research Council, who funded the GDS experiment in Kenya, and provided D.B. with a studentship, the Kenya Government for their permission to carry out the survey, and all the people who assisted with the field work, particularly Roger Young.

## References

- ANDERSON, D. L., SAMMIS, C. & JORDAN, T. 1972. Composition of the mantle and core. In: ROBERTSON, E.C. (ed.). *The Nature of the Solid Earth*. McGraw-Hill, 41-66.
- BAKER, B. H. & WOHLBERG, J. 1971. Structure and evolution of the Kenya rift valley. *Nature*, Londn. 229, 538-42.
- , MOHR, P. A. & WILLIAMS, L. A. J. 1972. Geology of the eastern rift system of Africa. *Spec. Pap. geol. Soc. Am.* 1.
- BANKS, R. J. & OTTEY, P. 1974. Geomagnetic deep sounding in and around the Kenya rift valley. *Geophys. J.R. astr. Soc.* 36, 321-35.
- BEAMISH, D. 1977. The mapping of induced currents around the Kenya Rift: a comparison of techniques. *Geophys. J. R. astr. Soc.* 50, 311-32.
- BIRCH, F. 1961. The velocity of compressional waves in rocks to 10 kilobars, part 2. *J. geophys. Res.* 66, 2199-224.
- FAIRHEAD, J. D. 1970. The structure of the lithosphere beneath the eastern rift, East Africa, deduced from gravity studies. *Tectonophysics* 30, 269-98.
- GRIFFITHS, D. H., KING, R. F., KIBAN, M. A. & BLUNDELL, D.J. 1971. Seismic refraction line in the Gregory rift. *Nature, Phys. Sci.* 229, 66-71.
- GURBUZ, C. 1974. The magnitude determination of local earthquake. in East Africa. Thesis, M.Sc., Univ. of Durham (unpubl.).
- KING, B. C. 1978. Structural and volcanic evolution of the Gregory Rift Valley, In: BISHOP, W. W. (ed.) *Geological Background to Fossil Man*. Scottish Academic Press, 29- 54.
- KNOPOFF, L. & SCHLUE, J. W. 1972. Rayleigh wave phase velocities for the path Addis Ababa-Nairobi. *Tectonophysics* 15, 157-63.
- LONG, R. E., BACKHOUSE, R. W., MAGUIRE, P. K. H. & SUNDARLINGHAM, K. 1972. The structure of East Africa using surface wave dispersion and Durham seismic array data. *Tectonophysics* 15, 165-178.
- LONG, R. E. & BACKHOUSE, R. W., 1976. The structure of the western flank of the Gregory Rift. Part H: The mantle. *Geophys. J.R. astr. Soc.* 44, 677-88.
- MAGUIRE, P. K. H. & LONG, R. E. 1976. Structure on the western flank of the Gregory Rift (Kenya). Part I: The crust. *Geophys. J.R. astr. Soc.* 44, 661-75.
- McCALL, G. J. H. 1970. Gabbroic and ultramafic nodules; high level intracrustal nodular occurrences in alkalic and associated volcanics from Kenya, described and compared with those from Hawaii. *Phys. Earth & Planet. Interiors* 3, 255-72.

MORGAN, P. 1974. *Terrestrial heat flow studies in Cyprus and Kenya*. Thesis, Ph.D., Imperial College, London Univ. (unpubl.).

ROONEY D. & HUTION. V. R. s. 1977. A magnetotelluric and magnetovariational study of the Gregory Rift, Kenya. *Geophys. J.R. astr. Soc.* 51, 91-119.

SEARLE, R. C. 1970. Evidence from gravity anomalies for thinning of the lithosphere beneath the rift valley in Kenya. *Geophys. J.R. astr. Soc.* 21, 13-31.

WAFF, H. S. 1974. Theoretical considerations of electrical conductivity in a partially molten mantle and implications for geothermometry. *J. geophys. Res.* 79, 4003- 10.

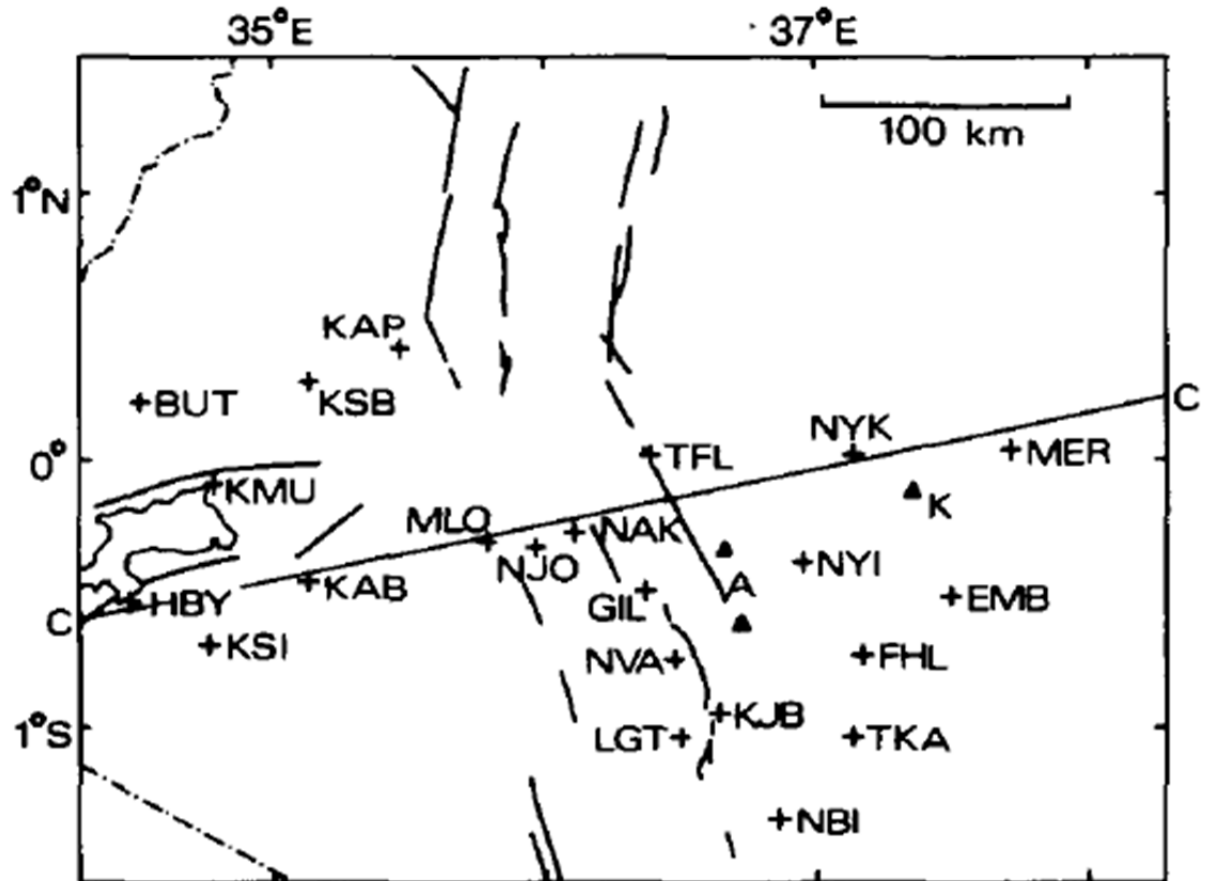


FIG. 1. Location of magnetometer sites in relation to the major rift faults. Mount Kenya (K) and the Aberdare mountains (A) are also shown.

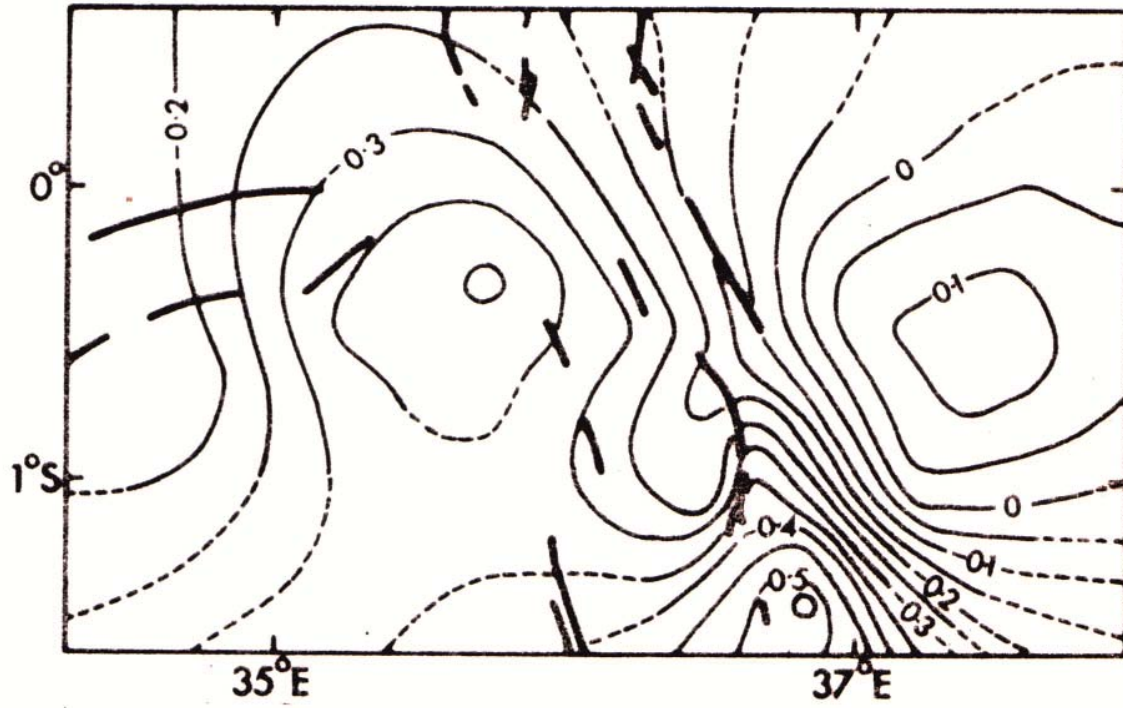


FIG. 2. The vertical fields (in-phase component) produced by anomalous internal currents when the azimuth of the regional horizontal field is  $60^\circ\text{E}$ , and its amplitude is  $1\text{nT}$ . Results shown are for frequency band 4 (periods of 16-32 min). Contour interval is  $0.05\text{ nT}$ .

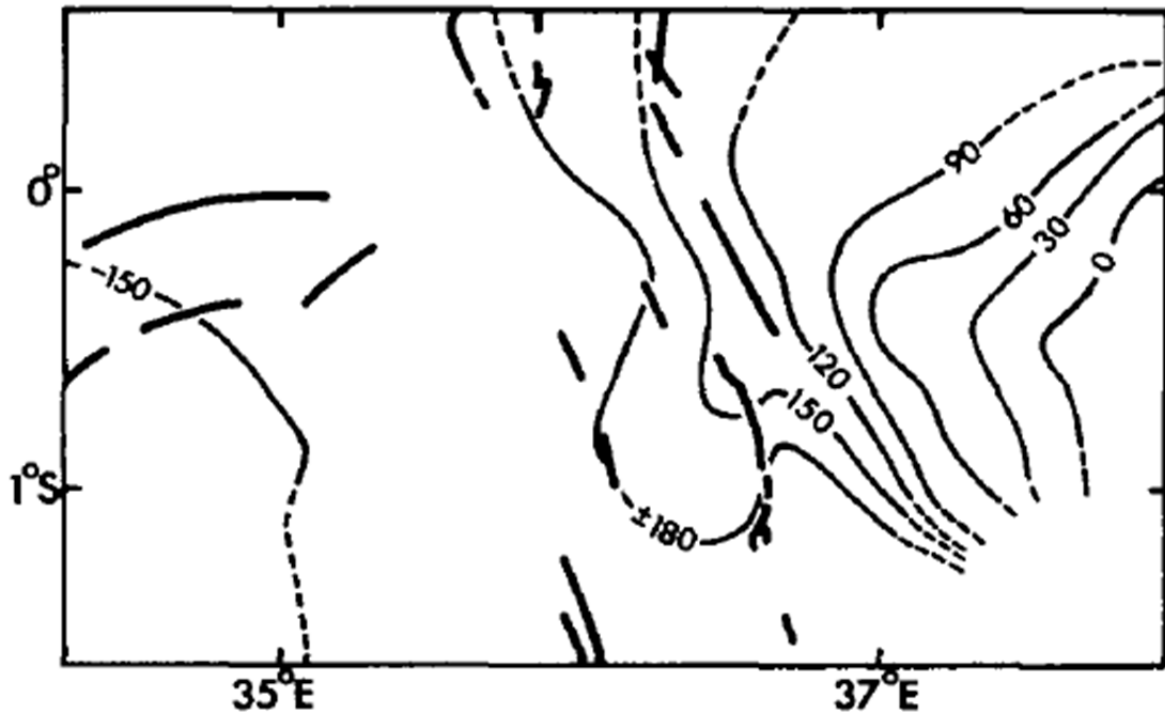


FIG. 3. The vertical field phase. The contour inter-val is  $30^\circ$ . No attempt has been made to contour across the phase discontinuity at  $\pm 180^\circ$ . Other details as for Fig. 2.

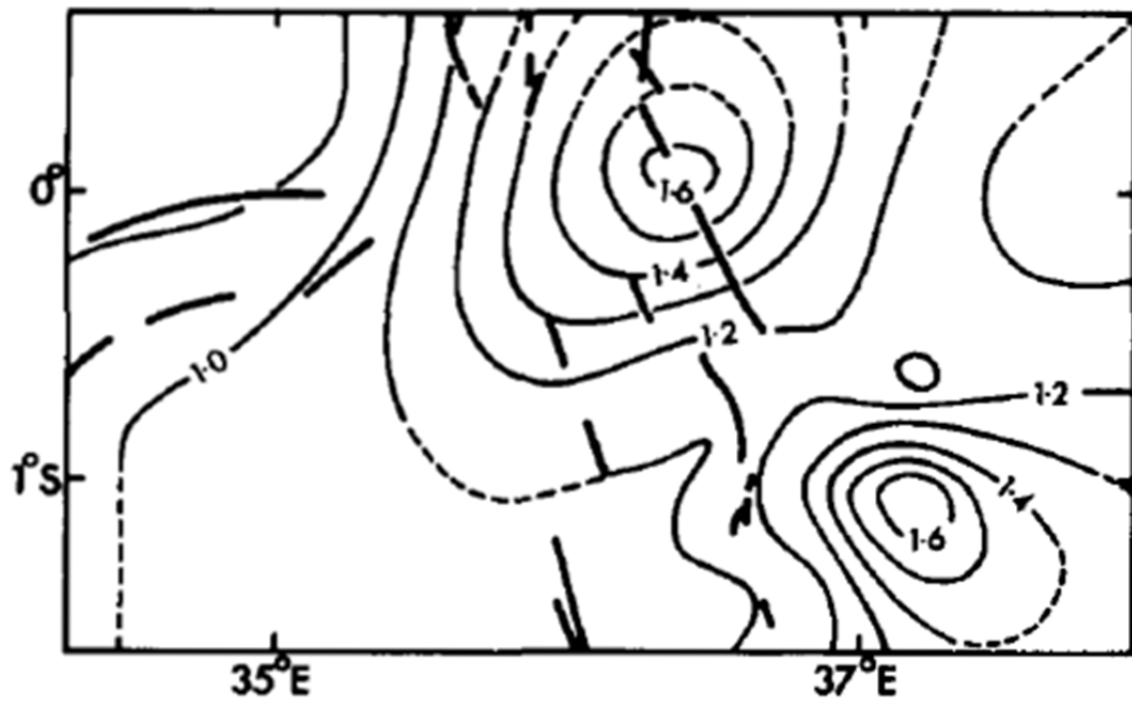


FIG. 4. The horizontal E field produced when the regional horizontal field azimuth is  $90^{\circ}\text{E}$ , and its amplitude is 1 nT. Contour interval is 0.1 nT. Other details as for Fig. 2.



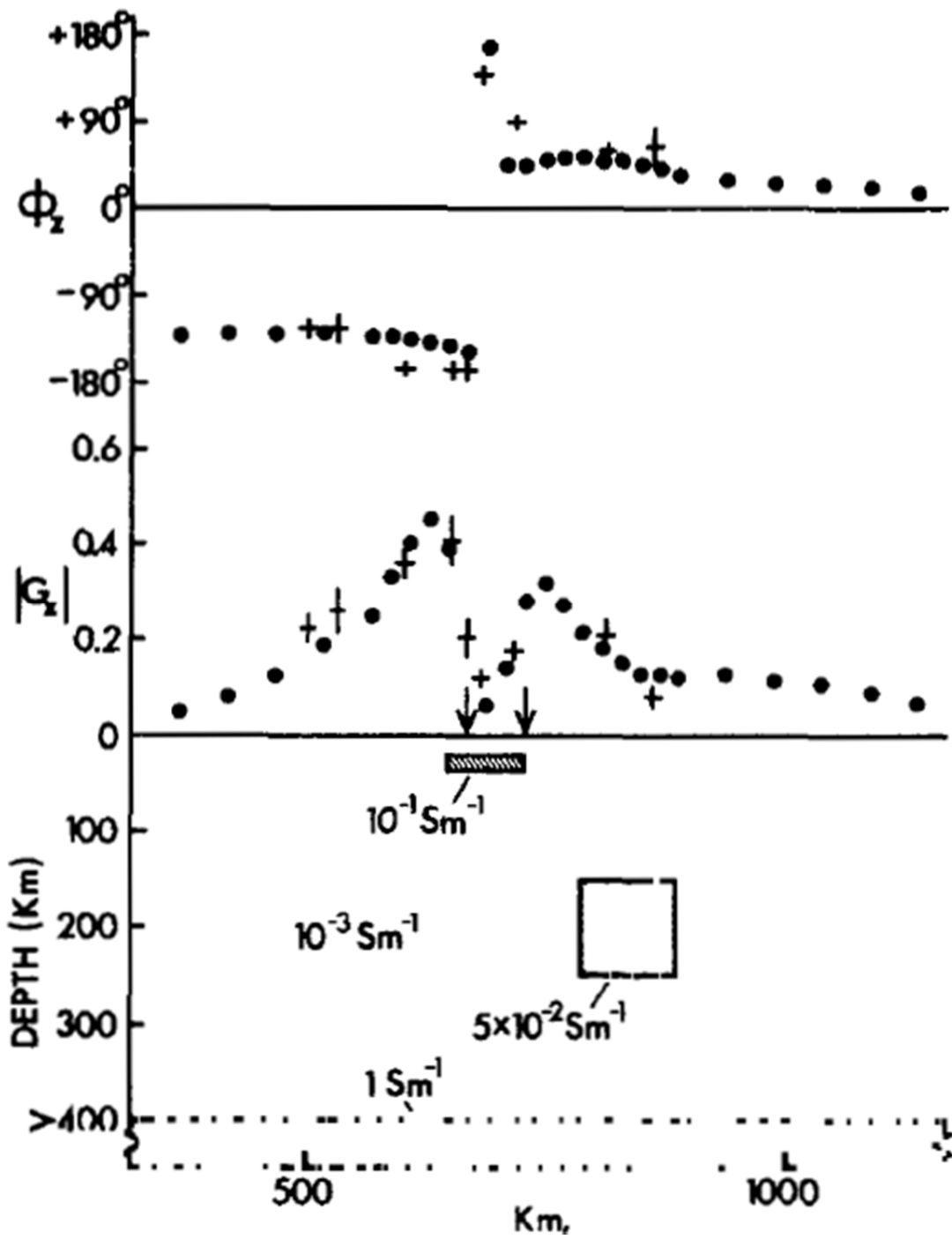


FIG. 5. Comparison between the observed single station vertical field responses along profile CC (Fig. 1), and the theoretical response of the conductivity structure shown. Crosses are observed values (vertical bars indicate errors); dots are theoretical values. Frequency band 4

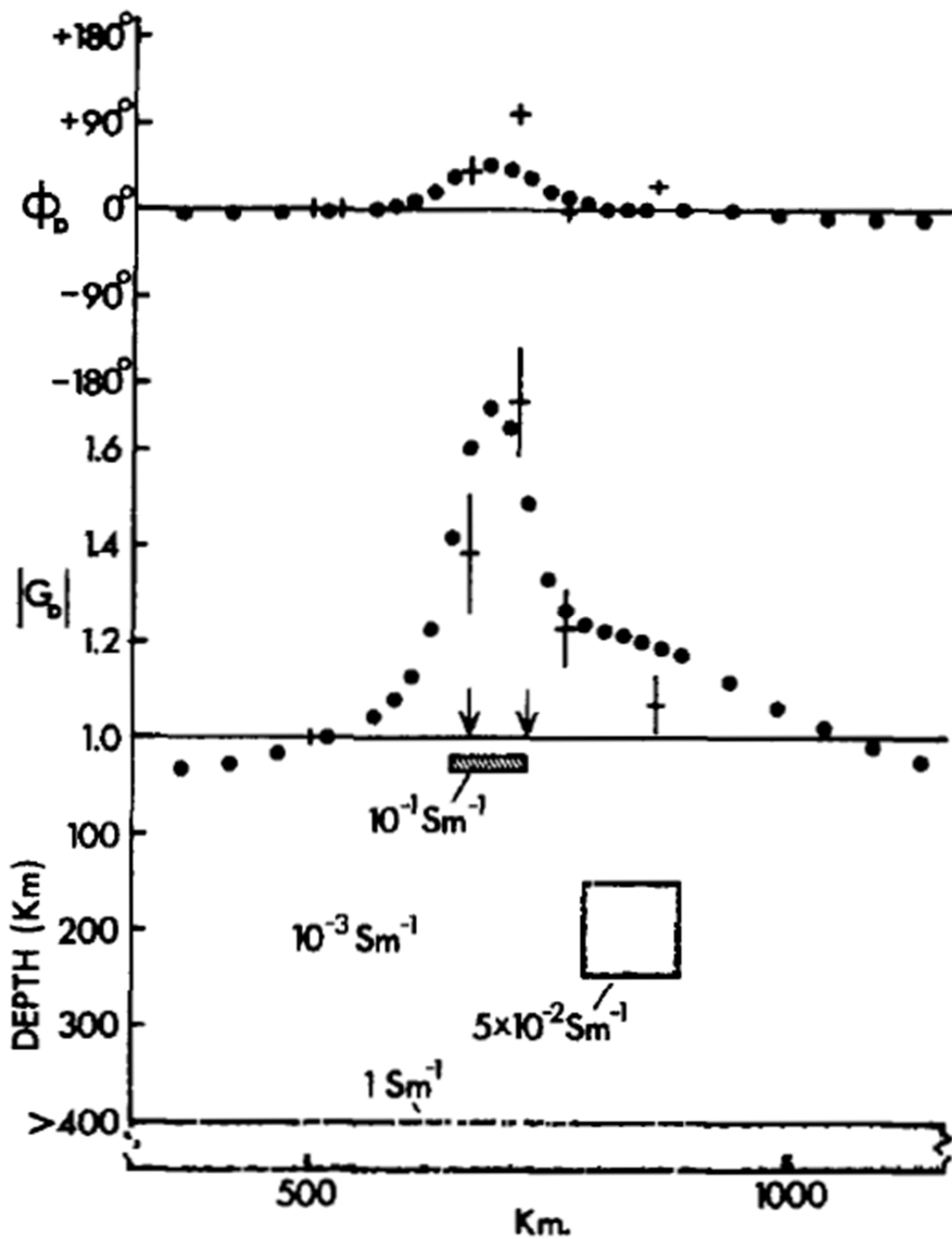


FIG. 6. Comparison between the observed and theoretical horizontal interstation responses. Details as for Fig. 5.

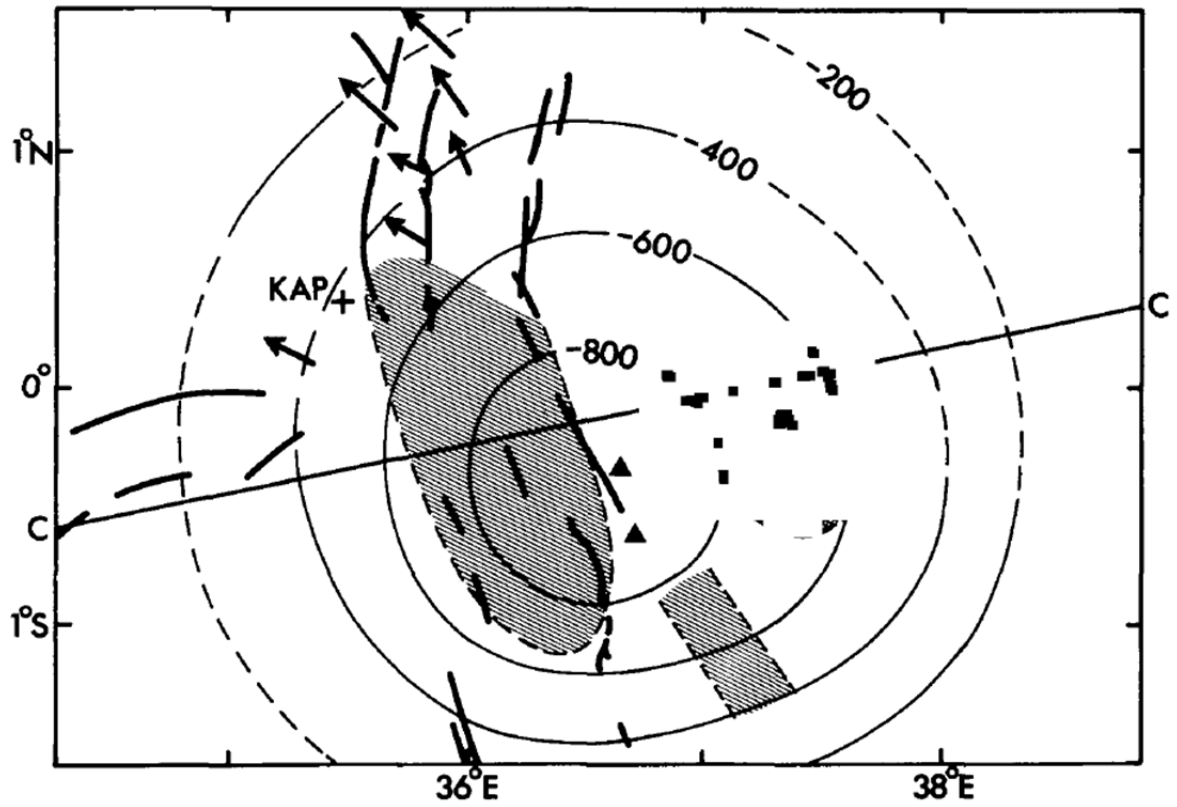


Fig. 7. Relationship of the conductivity anomalies (shaded areas) to other geophysical anomalies associated with the Kenya dome. Cross-hatching indicates a deep conductor; the others are shallow. The arrows show P-wave slowness anomalies measured at Kaptagat (KAP). The contours are estimates of the long wavelength Bouguer gravity anomaly specifically associated with the dome (values in  $\mu\text{m s}^{-2}$ ).